SPANDIDOS PUBLICATIONS

ONCOLOGY LETTERS 23: 161, 2022

Carboxymethylated pachyman induces ferroptosis in ovarian cancer by suppressing NRF1/HO-1 signaling

TIANTIAN JING, YANLI GUO and YANQIU WEI

Department of Gynecology, Tengzhou Central People's Hospital, Tengzhou, Shandong 277500, P.R. China

Received December 13, 2021; Accepted January 31, 2022

DOI: 10.3892/ol.2022.13281

Abstract. Carboxymethylated pachyman (CMP) is characterized by immune regulatory, antitumor and antioxidant activities. However, whether CMP contributes to the treatment of ovarian cancer has yet to be explored. The role of CMP in ovarian cancer cell death was analyzed using CCK-8 and flow cytometry assays. The data showed that CMP induced ovarian cancer cell death in a dose-dependent manner. Furthermore, CMP-induced cell death could be largely reversed by preincubation with ferrostatin-1 (Fer-1) but not 3-methyladenine or necrostatin-1. Reverse transcription-quantitative PCR analysis indicated that CMP significantly increased prostaglandin-endoperoxide synthase 2 (PTGS2) and Chac glutathione specific γ-glutamylcyclotransferase 1 (CHAC1) mRNA levels, but preincubation with Fer-1 obviously reduced PTGS2 and CHAC1 mRNA levels in SKOV3 and Hey cells. The intracellular levels of superoxide dismutase (SOD), glutathione (GSH), malondialdehyde (MDA) and Fe^{2+} were then quantified The data showed that 100 and 200 μg/ml CMP enhanced the production of SOD, MDA and Fe^{2+} but decreased GSH levels in SKOV3 and HEY cells. These data indicated that CMP could induce ferroptosis in ovarian cancer cells. More importantly, *in vitro* and *in vivo* studies indicated that CMP significantly suppressed nuclear factor erythroid 2-related factor 2 (Nrf2), heme oxygenase-1 (HO-1), cystine/glutamate antiporter system X(c)(-) (xCT) and glutathione peroxidase 4 (GPX4) expression in ovarian cancer cells and tumors. In conclusion, the present study showed novel data that CMP could induce ferroptotic death in ovarian cancer cells by suppressing Nrf2/HO-1/xCT/GPX4. All these findings indicate that CMP may have great potential in anti-ovarian cancer cell therapy by inducing ferroptosis.

Introduction

Ovarian cancer ranks the most lethal gynecologic malignancy and is now the second leading cause of death in women around the world (1,2). It has been reported that <50% of patients survive for >5 years after diagnosis (3). Ovarian cancer affects women of all ages but is most commonly diagnosed after menopause (4). Since early-stage disease is typically asymptomatic and symptoms of late-stage disease are nonspecific, >75% of affected women are diagnosed at an advanced stage (5-7). Therefore, it is important to explore the risk factors at the early stage.

Ferroptosis is a unique iron-dependent nonapoptotic cell death that is driven by depletion of glutathione (GSH) and accumulation of lipid reactive oxygen species (ROS) (8). Recently, elevated expression of nuclear factor erythroid 2-related factor 2 (Nrf2) was identified as an antioxidant transcription factor that defends malignant cells from ferroptosis (9). There are a number of different downstream effectors that are regulated by Nrf2, including heme oxygenase-1 (HO-1), glutathione peroxidase 4 (GPX4) and the cystine/glutamate antiporter system X(c)(-) (xCT) (10,11). HO-1 is associated with the endogenous antioxidant system and is an important member of the defense system (12). HO-1 can be activated by Nrf2, which subsequently eliminates hydroxyl-free radicals and excessive oxidation of lipids (12). xCT and GPX4 are two key regulators of ferroptosis (13). Downregulation of xCT and GPX4 can decrease intracellular cystine concentrations and lipid peroxide degradation, thereby leading to the accumulation of intracellular lipid peroxide and subsequent ferroptosis (13,14). Therefore, targeting the Nrf2 system may represent a potential therapeutic target for the treatment of ovarian cancer.

Carboxymethylated pachyman (CMP) is a carboxymethylated derivative of pachyman isolated from *Poria cocos* (Chinese name: Fu Ling) (15). Studies have demonstrated that CMP is characterized by immune regulatory, antitumor and antioxidant activities (15,16). For instance, CMP can improve colon injuries induced by 5-fluorouracil in CT26 tumor-bearing mice by regulating the NF-κB, Nrf2-ARE and MAPK/P38 pathways (16). However, whether CMP could contribute to the treatment of ovarian cancer remains to be elucidated.

Materials and methods

Cell culture. The ovarian cancer cell lines Hey and SKOV3 were purchased from Procell Life Science & Technology Co., Ltd. A human normal ovarian epithelial cell line (IOSE80) was purchased from BioVector NTCC, Inc. Cell line authentication was performed using short tandem repeats. Hey and SKOV3 cells were maintained in DMEM (HyClone; Cytiva) supplemented with 10% fetal bovine serum (FBS; HyClone; Cytiva)

Correspondence to: Dr Yanqiu Wei, Department of Gynecology, Tengzhou Central People's Hospital, 181 Xingtan Road, Tengzhou, Shandong 277500, P.R. China
E-mail: zxcv000987@yeah.net

Key words: ovarian cancer, ferroptosis, carboxymethylated pachyman, nuclear factor erythroid 2-related factor 2, heme oxygenase-1

and 1% antibiotics (penicillin and streptomycin; HyClone; Cytiva). IOSE80 cells were cultured in 90% RPMI-1640 medium (HyClone; Cytiva) and 10% FBS (HyClone; Cytiva). All cells were maintained in an incubator and 5% CO_2 at 37˚C.

CCK-8 assay. In brief, SKOV3 and Hey cells were seeded in 96-well plates at a density of 3,000 cells/well overnight at 37˚C. Thereafter, SKOV3 and Hey cells were incubated with 100, 200, 300, 400 and 500 μg/ml CMP for 24 h at 37˚C. Then, 10 μl CCK-8 (Beijing Solarbio Science & Technology Co., Ltd.) was added to each well and incubated at 37˚C for 4 h. The absorbance was determined at 450 nm using a microplate reader (Thermo Fisher Scientific, Inc.).

Annexin-PE/7-AAD assay. SKOV3 and Hey cells were seeded in 6-well plates at a density of 10,000 cells/well overnight at 37˚C. Then, SKOV3 and Hey cells were treated with 100 and 200 μg/ml CMP for 24 h at 37˚C. Cell death was analyzed using an Annexin V-PE/7-AAD Apoptosis Detection kit (cat. no. WE0328; Beijing Biolab Technology Co., Ltd.) according to the manufacturer's instructions. In brief, the cells were centrifuged at 1,000 x g for 5 min at 37˚C and collected. Then, 250 μl binding buffer was added, and the cell density was adjusted to 10^6 cells/ml. Next, the cells were incubated with 5 μl Annexin V-PE and 10 μl 7-AAD for 15 min at room temperature. Subsequently, 400 μl PBS was added, and the data were analyzed using a CytoFLEX V2-B4-R2 flow cytometer (cat. no. C02945; Beckman Coulter, Inc.). The data [early (Q3) + late (Q2) apoptotic cells] were analyzed using FlowJo v10 (FlowJo LLC).

Reverse transcription-quantitative PCR (RT-qPCR). SKOV3 and Hey cells were seeded in 6-well plates at a density of 10,000 cells/well overnight at 37˚C. Then, SKOV3 and Hey cells were treated with 100 and 200 μg/ml CMP for 24 h at 37˚C in the presence or absence of ferrostatin-1 (Fer-1, MCE). Total RNA was isolated from SKOV3 and Hey cells using RNAVzol LS (Vigorous Biotechnology Beijing Co., Ltd.) according to the manufacturer's protocol. The concentration and purity of RNA samples were determined by measuring the optical density (OD) 260/OD280.

RT-PCR was performed using a Takara PrimeScript One Step RT-PCR kit (Takara Bio, Inc.) according to the manufacture's protocols with three experiments replicated. The PCR amplifications were performed in a 50-μl reaction system containing 20 μl RNase Free ddH_2O, 25 μl 2X Step Buffer, 2 μl PrimeScript 1 Step Enzyme Mix, 1 μl upstream primer (1 μM), and 1 μl downstream primer (1 μM). The PCR was as follows: 50˚C for 30 min; 94˚C for 2 min; and 30 cycles of 94˚C for 30 sec, 55˚C for 30 sec, 72˚C for 1 min. GAPDH was used as an internal control using the $2^{-\Delta\Delta Cq}$ method (17). The primers were designed using Primer-BLAST (https://www.ncbi.nlm.nih.gov/tools/primer-blast/index.cgi?LINK_LOC=BlastHome) and the sequences were listed in Table I.

Table I. Primers used in the present study.

Primer name	Sequence (5'-3')
CHAC1-F	CCCCATCCTGGAACTTGACC
CHAC1-R	CTATGGATGGCTGGGCTGAG
PTGS2-F	GAGGGATCTGTGGATGCTTCG
PTGS2-R	AAACCCACAGTGCTTGACAC
NRF2-F	AAAGTGGCTGCTCAGAATTGC
NRF2-R	TTGCCATCTCTTGTTTGCTGC
HO-1-F	AGGGAATTCTCTTGGCTGGC
HO-1-R	GCTGCCACATTAGGGTGTCT
GAPDH-F	TTGCCCTCAACGACCACTTT
GAPDH-R	TGGTCCAGGGGTCTTACTCC

F, forward; R, reverse; CHAC1, Chac glutathione specific γ-glutamylcyclotransferase 1; PTGS2, prostaglandin-endoperoxide synthase 2; Nrf2, nuclear factor erythroid 2-related factor 2; HO-1, heme oxygenase-1.

Western blotting. Total proteins were isolated from SKOV3 and Hey cells using a total protein extraction kit (Beijing Solarbio Science & Technology Co., Ltd.) and collected following centrifugation at 12,000 x g for 30 min at 4˚C. A BCA protein assay kit (Pierce; Thermo Fisher Scientific, Inc.) was used to determine the protein concentration. A total of 20 μg protein was separated using 12% SDS-PAGE (F15012Gel; ACE Biotechnology Co., Ltd.), transferred onto polyvinylidene difluoride membranes (Pierce; Thermo Fisher Scientific, Inc.) and blocked with 5% fat-free milk at room temperature for 2 h. The membrane was incubated with the following primary antibodies: Nrf2 (cat. no. 12721; 1:1,000; Cell Signaling Technology, Inc.), HO-1 (cat. no. Ab52947; 1:1,000; Abcam), xCT (cat. no. 12691 for human, cat. no. 98051 for mouse; 1:1,000; Cell Signaling Technology, Inc.), GPX4 (cat. no. ab125066; Abcam) and GAPDH (cat. no. 5174; Cell Signaling Technology, Inc.), at 4˚C overnight. Then, the membranes were washed with PBST thrice. Next, the membrane was incubated with horseradish peroxidase (HRP)-conjugated goat anti-rabbit IgG (both 1:5,000; cat. no. ZB-2301; OriGene Technologies, Inc.) for 2 h at room temperature. Enhanced chemiluminescence (MilliporeSigma) was used to determine the protein concentrations according to the manufacturer's protocol. Signals were detected using a Super ECL Plus kit (Nanjing KeyGen Biotech Co., Ltd.) Quantitative analysis was performed using UVP 7.0 software (UVP LLC). Relative protein expression was normalized to GAPDH. All experiments were repeated thrice. ImageJ v1.43b software (National Institutes of Health) was used for densitometry analysis.

Quantification of Fe^{2+}, superoxide dismutase (SOD), glutathione (GSH) and malondialdehyde (MDA). The intracellular levels of Fe^{2+}, MDA, SOD and GSH were determined using colorimetric assay kits, including an iron assay kit (cat. no. EC-BC-K304-S; Elabscience Biotechnology, Inc.), Lipid Peroxidation MDA Assay kit (cat. no. A003-1; Nanjing Jiancheng Biotechnology Co. Ltd.), superoxide dismutase (SOD) Assay kit (cat. no. A001-3-1; Nanjing Jiancheng Biotechnology Co. Ltd.) and Reduced Glutathione Assay kit (cat. no. A005-1; Nanjing Jiancheng Biotechnology Co. Ltd.) according to the manufacturer's instructions.

DCFH-DA (2,7-Dichlorodi-hydrofluorescein diacetate) staining. SKOV3 and Hey cells were seeded in 6-well plates at a density of 10,000 cells/well overnight. Then, SKOV3 and

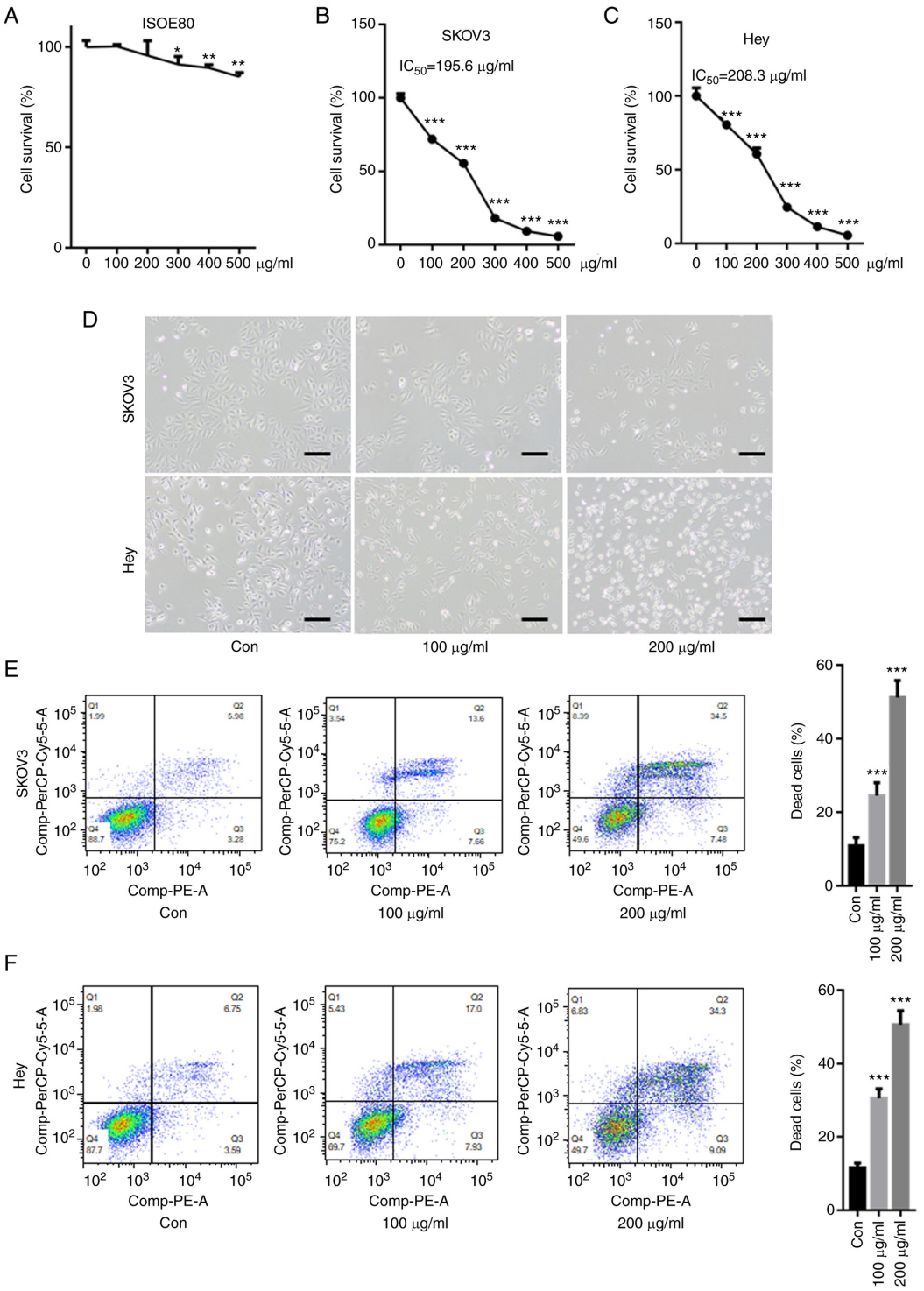

Figure 1. CMP induces cell death in SKOV3 and Hey cells. SKOV3 and Hey cells were incubated with CMP at different concentrations for 24 h. (A) 100 and 200 μg/ml CPM did not significantly decreased cell survival of IOSE80, but 300, 400, 500 μg/ml CPM slightly reduced IOSE80 cell survival rate. The CCK-8 assay showed that CMP significantly reduced the cell survival rate in (B) SKOV3 and (C) Hey cells in a dose-dependent manner. (D) Optical microscopy images demonstrated that 100 and 200 μM CMP obviously reduced cell viability and increased death cells in SKOV3 and Hey cells (scale bar=10 μM). SKOV3 and Hey cells were incubated with 100 and 200 μg/ml CMP for 24 h. The annexin V-PE/7-AAD assay indicated that 100 and 200 μg/ml CMP significantly enhanced (E) SKOV3 and (F) Hey cell death. *P<0.05, **P<0.01, ***P<0.001 vs. control. CMP, carboxymethylated pachyman; Con, control.

Hey cells were treated with 100 and 200 μg/ml CMP for 24 h at 37˚C. Then, the cells were incubated with 1 ml DCFH-DA (1:1,000) at room temperature for 20 min. Cells were washed with DMEM culture without FBS thrice. Representative images were obtained under a fluorescence microscope (magnification, x20; CKX53; Olympus Corporation).

In vivo assay. A total of eight nude female BALB/cA-nu mice (6 weeks old, weighing 20.1±1.8 g) were purchased from SPF (Beijing) Biotechnology Co., Ltd. (n=4 per group). The mice were kept in a 12 h light/dark cycle with controlled humidity (50-70%) and temperature (20-24˚C) with free access to food and water. They were randomly assigned to two experimental groups

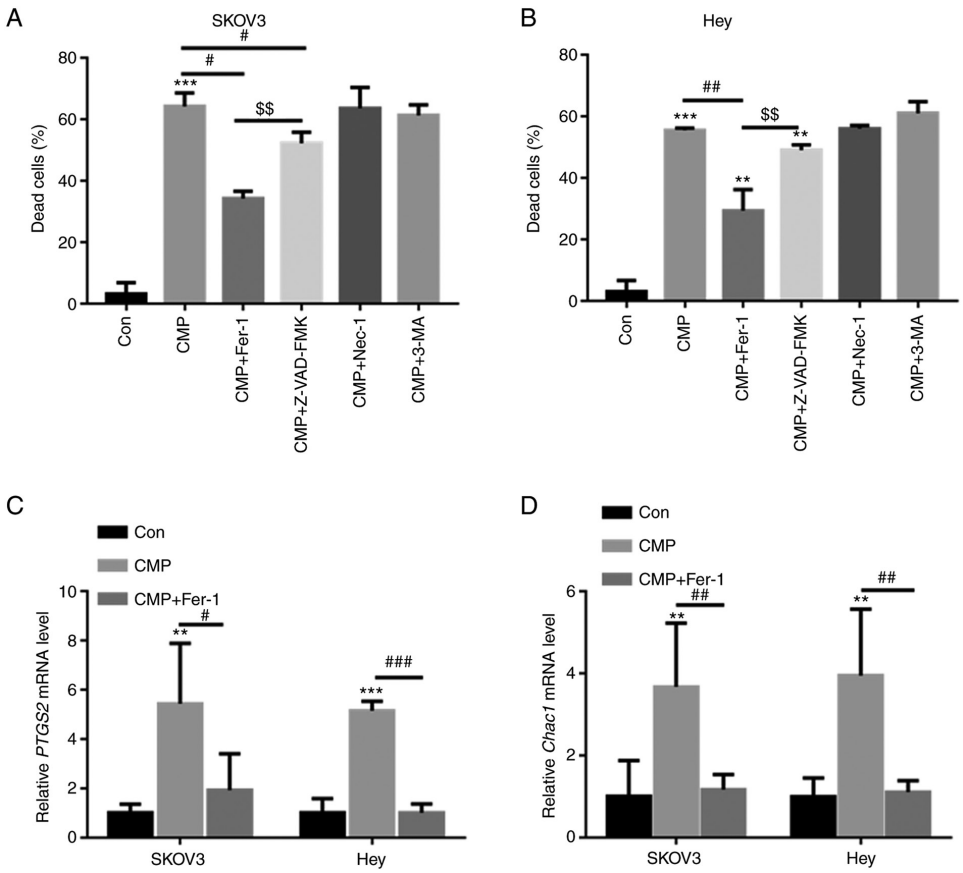

Figure 2. CMP induces ferroptosis in SKOV3 and Hey cells. SKOV3 and Hey cells were preincubated with 1 mM Fer-1, 10 mM Z-VAD-FMK, 10 mM 3-MA and 10 mM Nec-1 for 1 h. Then, the cells were treated with 100 μg/ml CMP for 24 h. Cell death was quantified using a CCK-8 assay in (A) SKOV3 and (B) Hey cells. Quantitative PCR analysis indicated that CMP significantly increased PTGS2 and CHAC1 mRNA levels, but preincubation with Fer-1 obviously reduced (C) PTGS2 and (D) CHAC1 mRNA levels in SKOV3 and Hey cells. **P<0.01, ***P<0.001 vs. con; $^{\#}$P<0.05, $^{\#\#}$P<0.01, $^{\#\#\#}$P<0.001 vs. CMP; $^{\$\$}$P<0.01 vs. CMP+ZVAD. CMP, carboxymethylated pachyman; Fer-1, ferrostatin-1; Z-VAD, Z-VAD-fluoromethylketone; PTGS2, prostaglandin-endoperoxide synthase 2; CHAC1, Chac glutathione specific γ-glutamylcyclotransferase 1; Con, control.

(n=4 per group). All experiments were approved according to the Ethics Committee of Tengzhou Central People's Hospital (Tengzhou, China; approval number TZH2020AH6) and were performed according to the National Institute of Health guidelines. SKOV3 cells (2x10^6 cells in 100 μl PBS) were subcutaneously injected into the flanks of 6-week-old female nude mice to induce tumor formation. After 24 h, mice in the control group were orally administered distilled water (20 ml/kg, 1 time/day for 28 days). Mice in the therapy group were orally administered CMP (50 mg/kg, 1 time/day for 28 days). All mice were sacrificed 28 days after injection by resection of the decapitation under deep isoflurane anesthesia (5%) (1). The successful induction of anesthesia was confirmed by observation of the following parameters: respiration decreased in frequency and increased in depth, eyelid and cornea reflexes disappeared, muscle tension and the reflex response reduced, and no response to pain or other stimulation was exhibited. Tumor grafts were excised, weighed, and harvested for further analysis. Tumor diameters were measured at regular intervals, and the tumor volume was calculated using the following formula: volume = length x width^2/2.

Statistical analysis. All data were expressed as the mean ± standard deviation. Unpaired Student's t-test was used to compare the differences between the two groups. One-way analysis of variance followed by Turkey analysis was used to analyze differences among three or more groups. Statistical analysis was performed using GraphPad Prism 8.0 Software (GraphPad Software, Inc.). P<0.05 was considered to indicate a statistically significant difference.

Results

Carboxymethylated pachyman (CMP) induces ovarian cancer cell death. First, the cytotoxicity of CPM on a human normal ovarian epithelial cell line, IOSE80 was tested. As shown in Fig. 1A, 100 and 200 μg/ml CPM did not significantly decreased cell survival of IOSE80, but 300, 400, 500 μg/ml CPM slightly reduced IOSE80 cell survival rate. The CCK-8 assay showed that CMP significantly reduced the cell survival rate in SKOV3 and Hey cells in a dose-dependent manner (Fig. 1B and C). Compared with SKOV3 and Hey cells, CMP did not result in too much cytotoxicity in IOSE80 cells, indicating the drug was not toxic to normal cells. The IC_{50} values of CMP in SKOV3 and Hey cells were 195.6 and 208.3 μg/ml, respectively. Optical microscopy images demonstrated that 100 and 200 μM CMP clearly reduced cell viability and increased cell death in SKOV3 and Hey cells (Fig. 1D). Furthermore, flow cytometry assays suggested that the cell death of both SKOV3 and Hey cells after 100 and 200 μg/ml CMP treatment, respectively, was significantly increased compared with that of the control (Fig. 1E and F).

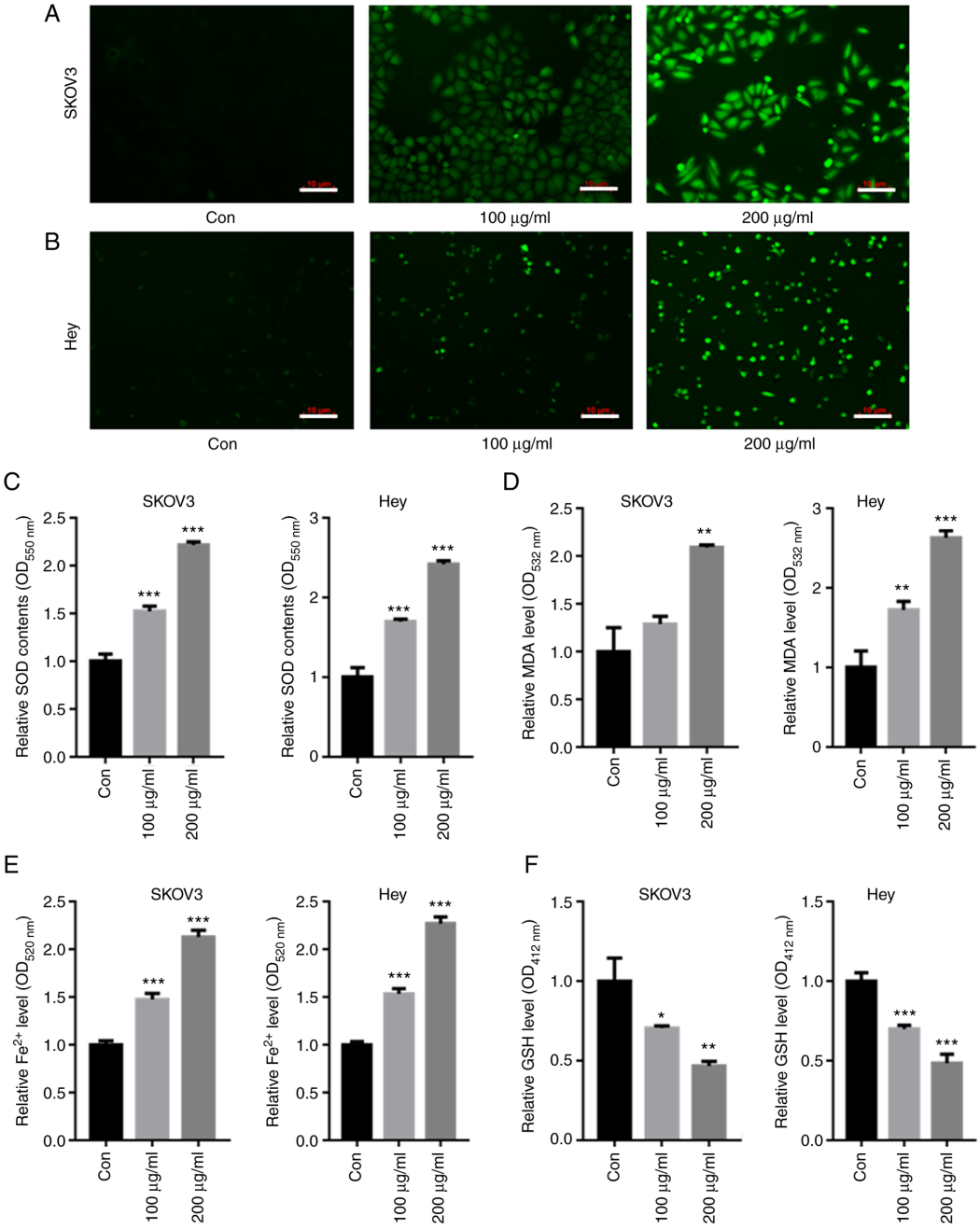

Figure 3. CMP upregulated intracellular ROS and Fe^{2+} in SKOV3 and Hey cells. SKOV3 and Hey cells were treated with 100 and 200 μg/ml CMP for 24 h. DCFH-DA staining showed that the intracellular ROS contents were enhanced in both (A) SKOV3 and (B) Hey cells treated with CMP (scale bar=10 μm). CMP enhanced the production of (C) SOD, (D) MDA and (E) Fe^{2+} but decreased the contents of (F) GSH in SKOV3 and Hey cells. *P<0.05, **P<0.01, ***P<0.001 vs. con. CMP, carboxymethylated pachyman; ROS, reactive oxygen species; DCFH-DA, 2,7-Dichlorodi-hydrofluorescein diacetate; SOD, superoxide dismutase; MDA, malondialdehyde; GSH, glutathione; Con, control.

CMP induces ferroptosis in SKOV3 and Hey cells. SKOV3 and Hey cells were preincubated with different inhibitors, including ferroptosis inhibitors (ferrostatin-1, Fer-1), apoptosis inhibitors (Z-VAD-fluoromethylketone, Z-VAD-FMK), autophagy inhibitors (3-methyladenine, 3-MA), and necrosis inhibitors (necrostatin-1, Nec-1). As shown in Fig. 2A and B, CMP-induced cell death was largely reversed by preincubation with Fer-1 and Z-VAD-FMK but was not abolished by Nec-1 and 3-MA. Z-VAD-FMK decreased CMP-induced cell death by ~6.4%, whereas Fer-1 reduced CMP-induced cell death by ~26.1% (Fig. 2A and B). The present study further evaluated the mRNA levels of PTGS2 and CHAC1, two important ferroptosis markers, in SKOV3 and Hey cells treated with CMP and Fer-1. RT-qPCR analysis indicated that CMP significantly increased PTGS2 and CHAC1 mRNA levels, but preincubation with Fer-1 obviously reduced PTGS2 and CHAC1 mRNA levels in SKOV3 and Hey cells (Fig. 2C and D). These data indicated that CMP could induce ferroptosis in ovarian cancer cells.

CMP upregulated intracellular SOD and Fe^{2+} in ovarian cancer cells. DCFH-DA staining showed that both 100 and 200 μg/ml CMP elevated the intracellular SOD contents compared with those of the control in both SKOV3 and Hey cells (Fig. 3A and B). The intracellular levels of SOD, GSH,

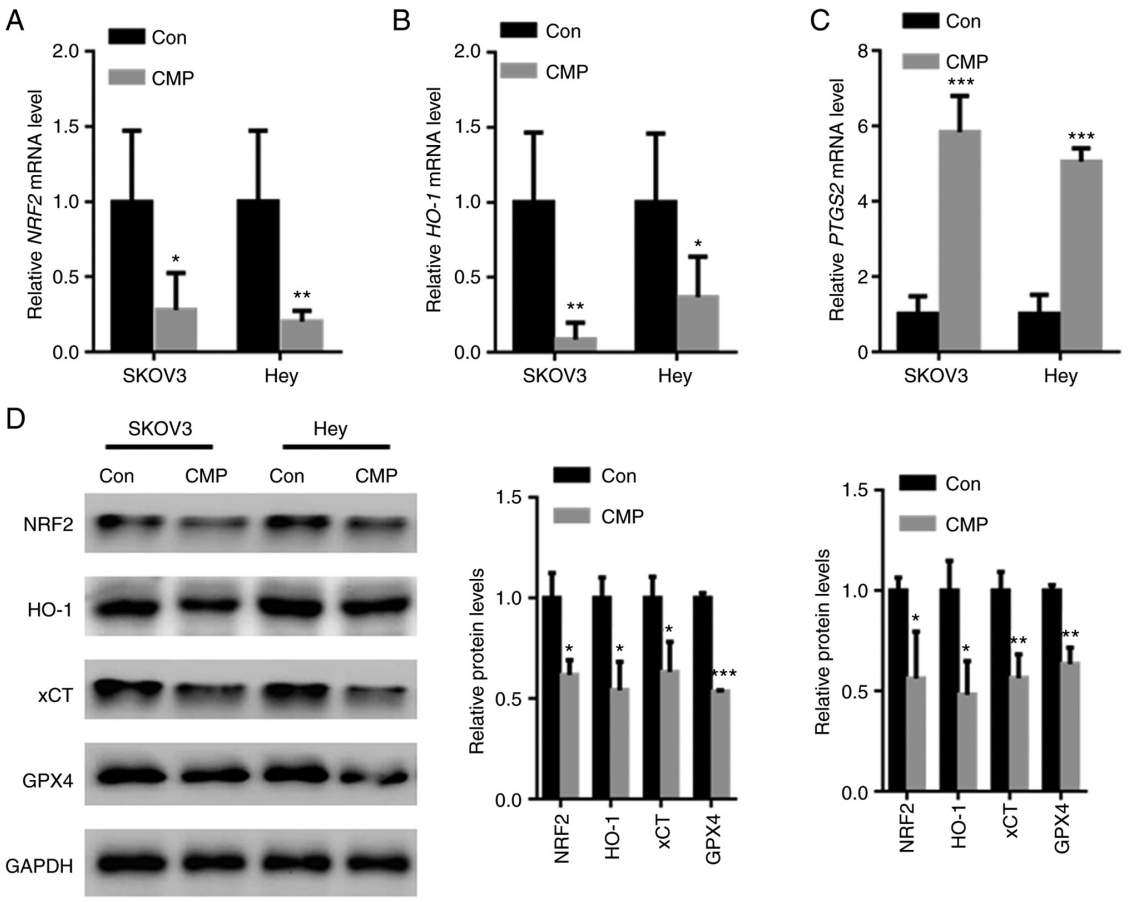

Figure 4. CMP induced ovarian cancer cell ferroptosis by downregulating Nrf2. SKOV3 and Hey cells were treated with 100 μg/ml CMP for 24 h. RT-PCR analysis showed that CMP reduced (A) Nrf2 and (B) HO-1 mRNA levels but increased the (C) PTGS2 mRNA levels. (D) CMP decreased the expression of Nrf2, HO-1, xCT and GPX4 in SKOV3 and Hey cells. *P<0.05, **P<0.01, ***P<0.001 vs. con. CMP, carboxymethylated pachyman; Nrf2, nuclear factor erythroid 2-related factor 2; HO-1, heme oxygenase-1; PTGS2, prostaglandin-endoperoxide synthase 2; xCT, cystine/glutamate antiporter system X(c)(-); Con, control.

MDA and Fe^{2+} were then quantified. The data showed that 100 and 200 μg/ml CMP enhanced the production of SOD, MDA and Fe^{2+} (Fig. 3C-E) but decreased GSH levels in SKOV3 and Hey cells (Fig. 3F).

CMP induced ovarian cancer cell ferroptosis by downregulating Nrf2. Nrf2-associated antioxidant stress plays a key role in ferroptosis inhibition (18). RT-qPCR analysis showed that CMP reduced Nrf2 and HO-1 mRNA levels but increased PTGS2 mRNA levels (Fig. 4A-C). In addition, the effects of CMP on the expression of Nrf2 and corresponding downstream target genes was tested. The data showed that Nrf2, HO-1, xCT and GPX4 protein levels were decreased in SKOV3 and Hey cells treated with CMP (Fig. 4D).

CMP decreased in vivo tumor growth by suppressing Nrf2-associated ferroptosis. In vivo assays showed that CMP significantly suppressed tumor volume and weight compared with those of the control (Fig. 5A-C). The intracellular contents of Fe^{2+}, MDA, SOD and GSH was further quantified. The data showed that CMP significantly increased the accumulation of Fe^{2+}, MDA, and SOD but reduced the levels of GSH (Fig. 5D-G). In addition, Nrf2, HO-1, xCT and GPX4 protein levels were suppressed in nude mice treated with CMP compared with those of the control (Fig. 5H).

Discussion

As the leading cause of death from gynecological malignancy worldwide, >75% of affected women are diagnosed at advanced stages of ovarian cancer with vague and nonspecific symptoms (7). Following diagnosis, the 5-year survival rate of late-stage patients is reported to be <33% (3). One novel promising anticancer treatment method is ferroptosis, which is a well-regulated cell death characterized by lipid peroxidation (19).

The antitumor effects of CMP have been identified in colon cancer and hepatocellular carcinoma (15,16). Consistent with these findings, the present study showed novel data that CMP significantly suppressed cell survival and induced cell death in ovarian cancer. To further analyze which form of cell death could be induced by CMP, ovarian cancer cells were preincubated with different inhibitors, including apoptosis inhibitors, ferroptosis inhibitors, necrosis inhibitors and autophagy inhibitors. The data showed that CMP-induced cell death could be significantly abolished by Fer-1, a ferroptosis inhibitor. In addition, CMP-induced upregulation of PTGS2 and CHAC1, two ferroptosis markers, was significantly decreased by preincubation with Fer-1. These findings indicated that CMP exhibited potent anticancer effects on ovarian cancer cells by inducing ferroptosis.

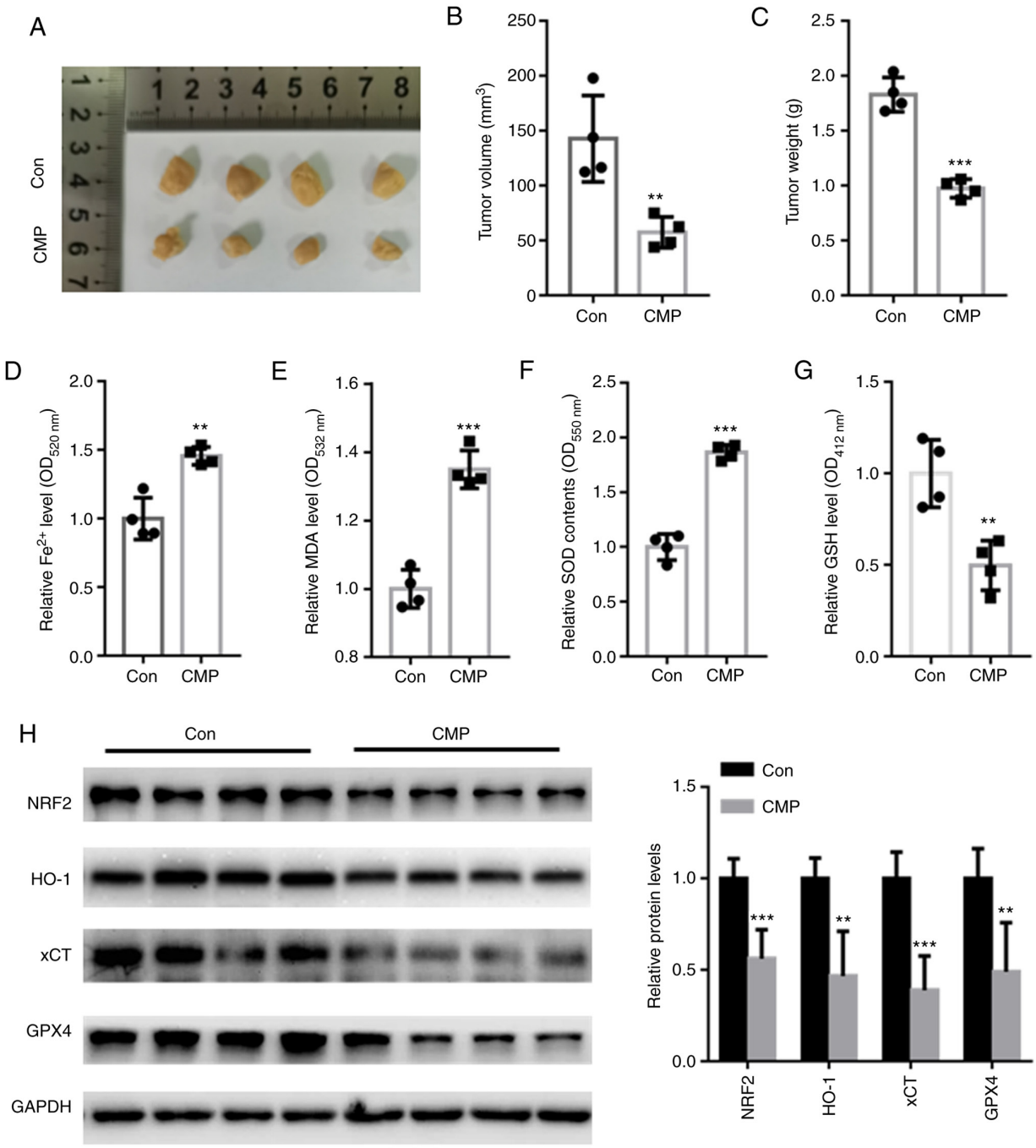

Figure 5. CMP (50 mg/kg, 1 time/day for 28 days) decreased *in vivo* tumor growth by suppressing NRF2-associated ferroptosis. (A) Representative tumor images. CMP significantly suppressed tumor (B) volume and (C) weight compared with those of the control. CMP significantly increased the accumulation of (D) Fe^{2+}, (E) MDA and (F) SOD but reduced the levels of (G) GSH. (H) Western blot assay showed that Nrf2, HO-1, xCT and GPX4 protein levels were suppressed in nude mice treated with CMP compared with those of the control. **P<0.01, ***P<0.001 vs. con. CMP, carboxymethylated pachyman; Nrf2, nuclear factor erythroid 2-related factor 2; MDA, malondialdehyde; SOD, superoxide dismutase; GSH, glutathione; HO-1, heme oxygenase-1; xCT, cystine/glutamate antiporter system X(c)(-); Con, control.

Upregulation of oxidative stress (ROS) levels is suggested to be a hallmark of ferroptosis (20). Hence, the effects of CMP on intracellular ROS production in ovarian cancer cells was evaluated. The data showed that CMP enhanced the production of ROS. CMP also enhanced iron levels and MDA contents in SKOV3 and Hey cells. GSH synthesis is mediated via xCT, which exchanges intracellular glutamate for extracellular cystine (20). As a major endogenous antioxidant, GPX4 protects cancer cells from ferroptosis by eliminating lipid hydroperoxide (20). Consistently, it was found that CMP decreased GSH in ovarian cancer cells, indicating that ovarian cancer cells are more vulnerable to ferroptosis under CMP treatment.

Oxidative damage induced via free radicals promotes the pathogenesis of multiple diseases, including cancer (21). The transcription factor nuclear factor Nrf2 renders cells resistant to cellular defense against toxic and oxidative insults by regulating genes involved in drug detoxification and antioxidant

defense responses (22). For instance, Nrf2-mediated activation of HO-1 is indicated to protect against oxidative stress (23). xCT is an important gene that participates in modulating 'iron overload-ferroptosis' (23). Decreased xCT expression leads to significant oxygen elevation and a reduction in intracellular antioxidant capacity (23). Silencing of Nrf2 has been shown to reduce xCT and HO-1 expression, thereby facilitating lipid peroxide production (23). In addition, Nrf2 also serves a key role in regulating the antioxidant system by involving iron metabolism and glutathione synthesis (24). Of note, GPX4, which suppresses the canonical ferroptosis pathway, is a downstream target gene of Nrf2 (25). Consistent with these findings, the present study found that CMP significantly suppressed Nrf2, HO-1, xCT and GPX4 expression in ovarian cancer cells and tumors. These observations suggested that CMP induced ferroptosis in ovarian cancer cells by suppressing the Nrf2/HO-1-mediated ferroptosis pathway.

However, there are limitations to the present study. First, it will be rewarding to see the results to be verified in human studies. Second, whether CMP suppresses the development of ovarian cancer via other molecular mechanisms deserves further study.

In conclusion, the present study produced novel data that CMP could induce ferroptotic cell death in ovarian cancer cells by suppressing Nrf2/HO-1/xCT/GPX4. All these findings indicated that CMP may have great potential in anti-ovarian cancer cell therapy by inducing ferroptosis.

Acknowledgements

Not applicable.

Funding

The present study was supported by a grant from Tengzhou Central People's Hospital (grant no. TZH-20190721).

Availability of data and materials

The datasets used and/or analyzed during the current study are available from the corresponding author on reasonable request.

Authors' contributions

TJ performed the experiments, analyzed the data and wrote the paper. YG performed part of the RT-qPCR experiments. YW designed the experiments, analyzed the data and gave final approval of the version to be published. TJ and YW confirm the authenticity of all the raw data All authors read and approved the final manuscript.

Ethics approval and consent to participate

The present study was approved by the Research Ethics Committee of Tengzhou Central People's Hospital (Tengzhou City, China; approval no. TZH2020AH6).

Patient consent for publication

Not applicable.

Competing interests

The authors declare that they have no competing interests.

References

1. Wang Y and Zhu Z: Oridonin inhibits metastasis of human ovarian cancer cells by suppressing the mTOR pathway. Arch Med Sci 15: 1017-1027, 2019.
2. Yang C, Xia BR, Zhang ZC, Zhang YJ, Lou G and Jin WL: Immunotherapy for ovarian cancer: Adjuvant, combination, and neoadjuvant. Front Immunol 11: 577869, 2020.
3. Doubeni CA, Doubeni AR, and Myers AE: Diagnosis and management of ovarian cancer. Am Fam Physician 93: 937-944, 2016.
4. Achatz MI, Caleffi M, Guindalini R, Marques RM, Nogueira-Rodrigues A and Ashton-Prolla P: Recommendations for advancing the diagnosis and management of hereditary breast and ovarian cancer in Brazil. JCO Glob Oncol 6: 439-452, 2020.
5. Jafari M, Hasanzadeh M, Solhi E, Hassanpour S, Shadjou N, Mokhtarzadeh A, Jouyban A and Mahboob S: Ultrasensitive bioassay of epitope of Mucin-16 protein (CA 125) in human plasma samples using a novel immunoassay based on silver conductive nano-ink: A new platform in early stage diagnosis of ovarian cancer and efficient management. Int J Biol Macromol 126: 1255-1265, 2019.
6. Johnson C and Jazaeri AA: Diagnosis and management of immune checkpoint inhibitor-related toxicities in ovarian cancer: A series of case vignettes. Clin Ther 40: 389-394, 2018.
7. Jayson GC, Kohn EC, Kitchener HC and Ledermann JA: Ovarian cancer. Lancet 384: 1376-1388, 2014.
8. Sun Y, Chen P, Zhai B, Zhang M, Xiang Y, Fang J, Xu S, Gao Y, Chen X, Sui X and Li G: The emerging role of ferroptosis in inflammation. Biomed Pharmacother 127: 110108, 2020.
9. Dodson M, Castro-Portuguez R and Zhang DD: NRF2 plays a critical role in mitigating lipid peroxidation and ferroptosis. Redox Biol 23: 101107, 2019.
10. Zhang H, Yuan B, Huang H, Qu S, Yang S and Zeng Z: Gastrodin induced HO-1 and Nrf2 up-regulation to alleviate H_2O_2-induced oxidative stress in mouse liver sinusoidal endothelial cells through p38 MAPK phosphorylation. Braz J Med Biol Res 51: e7439, 2018.
11. Fan Z, Wirth AK, Chen D, Wruck CJ, Rauh M, Buchfelder M and Savaskan N: Nrf2-Keap1 pathway promotes cell proliferation and diminishes ferroptosis. Oncogenesis 6: e371, 2017.
12. Li B, Nasser MI, Masood M, Adlat S, Huang Y, Yang B, Luo C and Jiang N: Efficiency of traditional Chinese medicine targeting the Nrf2/HO-1 signaling pathway. Biomed Pharmacother 126: 110074, 2020.
13. Chen D, Fan Z, Rauh M, Buchfelder M, Eyupoglu IY and Savaskan N: ATF4 promotes angiogenesis and neuronal cell death and confers ferroptosis in a xCT-dependent manner. Oncogene 36: 5593-5608, 2017.
14. Lee N, Carlisle AE, Peppers A, Park SJ, Doshi MB, Spears ME and Kim D: xCT-Driven expression of GPX4 determines sensitivity of breast cancer cells to ferroptosis inducers. Antioxidants (Basel) 10: 317, 2021.
15. Wang C, Huo X, Gao L, Sun G and Li C: Hepatoprotective effect of carboxymethyl pachyman in fluorouracil-treated CT26-bearing mice. Molecules 22: 756, 2017.
16. Wang C, Yang S, Gao L, Wang L and Cao L: Carboxymethyl pachyman (CMP) reduces intestinal mucositis and regulates the intestinal microflora in 5-fluorouracil-treated CT26 tumour-bearing mice. Food Funct 9: 2695-2704, 2018.
17. Livak KJ and Schmittgen TD: Analysis of relative gene expression data using real-time quantitative PCR and the 2(-Delta Delta C(T)) method. Methods 25: 402-408, 2001.
18. Qiang Z, Dong H, Xia Y, Chai D, Hu R and Jiang H: Nrf2 and STAT3 alleviates ferroptosis-mediated IIR-ALI by regulating SLC7A11. Oxid Med Cell Longev 2020: 5146982, 2020.
19. Carbone M and Melino G: Stearoyl Coa desaturase regulates ferroptosis in ovarian cancer offering new therapeutic perspectives. Cancer Res 79: 5149-5150, 2019.
20. Zhu J, Xiong Y, Zhang Y, Wen J, Cai N, Cheng K, Liang H and Zhang W: The molecular mechanisms of regulating oxidative stress-induced ferroptosis and therapeutic strategy in tumors. Oxid Med Cell Longev 2020: 8810785, 2020.
21. Oh YS and Jun HS: Effects of glucagon-like peptide-1 on oxidative stress and Nrf2 Signaling. Int J Mol Sci 19: 26, 2017.

22. Bellezza I, Giambanco I, Minelli A and Donato R: Nrf2-Keap1 signaling in oxidative and reductive stress. Biochim Biophys Acta Mol Cell Res 1865: 721-733, 2018.
23. Dong H, Qiang Z, Chai D, Peng J, Xia Y, Hu R and Jiang H: Nrf2 inhibits ferroptosis and protects against acute lung injury due to intestinal ischemia reperfusion via regulating SLC7A11 and HO-1. Aging (Albany NY) 12: 12943-12959, 2020.
24. Song X and Long D: Nrf2 and Ferroptosis: A new research direction for neurodegenerative diseases. Front Neurosci 14: 267, 2020.
25. Deng HF, Yue LX, Wang NN, Zhou YQ, Zhou W, Liu X, Ni YH, Huang CS, Qiu LZ, Liu H, *et al*: Mitochondrial iron overload-mediated inhibition of Nrf2-HO-1/GPX4 Assisted ALI-induced nephrotoxicity. Front Pharmacol 11: 624529, 2021.